

Use of a single-mode fiber coupler for second-harmonic-generation microscopy

Ling Fu, Xiaosong Gan, and Min Gu

Centre for Micro-Photonics, School of Biophysical Sciences and Electrical Engineering, Swinburne University of Technology, P.O. Box 218, Hawthorn, Victoria 3122, Australia

Received July 21, 2004

We present a compact second-harmonic-generation (SHG) microscope based on a three-port single-mode fiber coupler. The fiber coupler is used to deliver a near-infrared ultrashort-pulsed laser beam as well as to collect the SHG signal in the visible wavelength range. The SHG microscope exhibits an axial resolution of $1.8 \mu\text{m}$, which shows a slight enhancement of the optical sectioning effect compared with that for two-photon excitation at the same excitation wavelength. It is also demonstrated that SHG and two-photon fluorescence images under parallel and perpendicular laser excitation polarization can be simultaneously obtained.

© 2005 Optical Society of America

OCIS codes: 110.0180, 110.2350, 180.2520.

Although second-harmonic generation (SHG) was demonstrated almost as soon as the first laser was built, only more recently has it rapidly emerged as a powerful contrast mechanism in nonlinear microscopy.^{1–4} Like two-photon fluorescence microscopy, SHG microscopy possesses benefits that include an intrinsic optical sectioning property, reduced out-of-plane photobleaching and phototoxicity, and deeper penetration depth. In particular, because of its coherent scattering nature SHG facilitates direct imaging of highly polarizable and ordered noncentrosymmetric structures without exogenous molecular probes, and polarization anisotropy to extract nonlinear organization of samples. Therefore SHG imaging of endogenous proteins such as collagen, microtubules, and actomyosin in live tissue may provide a new angle for tissue morphology, cell–cell interaction, and diseases diagnosis.^{5,6}

At present, the majority of SHG studies of biological tissue are made with a transmitted detection geometry on a bench top with bulk optics that precludes *in vivo* applications to living animals. However, the integration of optical fiber components into an imaging system overcomes this limitation and may provide the ability to image tissue inside the body. Fiber-optic two-photon fluorescence microscopes and endoscopes that use single-mode fiber couplers have been reported.^{7,8} Compared with conventional two-photon fluorescence microscopy, fiber-optic two-photon fluorescence microscopy takes advantage of a compact arrangement, self-alignment, and an enhanced optical sectioning effect.^{9,10} Although the effectiveness of the fiber coupler has been demonstrated in two-photon fluorescence microscopy, the difficulty in adopting fiber-optic components in SHG microscopy is due to the fact that the wavelength range into which the SHG signal falls is farther away from the designed wavelength of the fiber-optic components than that of normal two-photon fluorescence. Moreover, polarization preservation of the illuminating laser beam and the collected SHG signal is essential for probing the orientation of structural proteins in tissues. In this Letter we present

what is to our knowledge the first fiber-optic SHG microscope that uses a three-port single-mode fiber coupler. We demonstrate that the new instrument can collect the SHG signal and two-photon fluorescence simultaneously and efficiently.

The experimental arrangement of the new SHG microscope is depicted in Fig. 1, which is similar to the system that was used before,⁷ except for the following modifications: The backscattering SHG signal is collected by the imaging objective and delivered via port 2 (signal arm) of the fiber coupler (Newport Model F-CPL-S12785) to a photomultiplier tube (PMT) for imaging or to a CCD-based fiber-coupled spectrograph (Acton Research Corporation) to collect spectra. An appropriate bandpass filter (BF) was placed in front of the PMT to ensure that only the SHG signal is detected. We switched between imaging and spectra acquisition by changing the direction of a flip mirror (FM).

The coupling efficiency from port 3 to port 1 is 20–41% in the wavelength range 770–870 nm, and that from port 2 to port 1 is 29–41% in the range 435–532 nm, as shown in inset (a) of Fig. 2 [the 435-nm laser beam is obtained by combination of the Ti:sapphire laser and a frequency doubler (Spectra-Physics), whereas the 532-nm laser beam is a

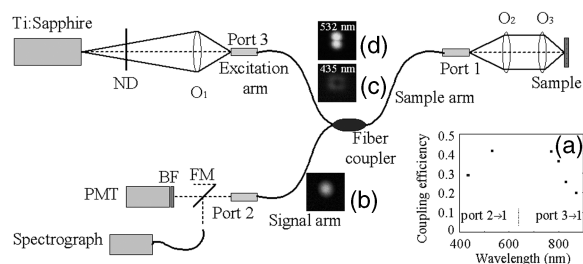


Fig. 1. Schematic diagram of the SHG microscope with a single-mode fiber coupler: (a) coupling efficiency from ports 2 and 3 to port 1; (b)–(d) mode profiles in the excitation and signal arms when a visible beam is coupled to port 1. ND, neutral density.

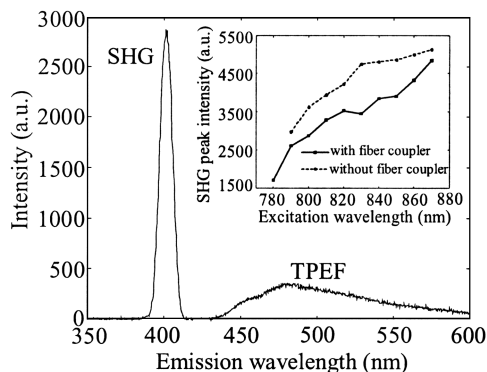


Fig. 2. Emission spectra of AF-50 dye at 800 nm. Inset, SHG peak intensity as a function of excitation wavelength. The solid curve in the inset is derived from the spectra collected by focusing the output beam from port 2 of the fiber coupler into the spectrograph; the dashed curve is derived from the spectra collected directly from the sample without use of the fiber coupler. The excitation power is approximately 4 mW on the sample, and the excitation polarization is parallel to the fundamental laser polarization. TPEF, two-photon-excited fluorescence.

continuous beam (Spectra-Physics Millennia)]. Consequently, a laser power of as much as 80–150 mW in the near-infrared wavelength range can be delivered to the imaging objective. Although the ultrashort-pulsed laser beam is broadened to a few picoseconds owing to group-velocity dispersion and self-phase modulation during delivery, sufficient power still can be achieved after propagation of the laser beam through the coupler.^{7–10}

To understand the propagation properties of the SHG signal, which is in the visible wavelength range, through the fiber coupler, we measured the mode profile and the coupling efficiency at ports 2 and 3 when beams at wavelengths of 435 and 532 nm, respectively, illuminated port 1. We found that, in both cases, the field distribution from port 2 remained as the single-mode profile illustrated in inset (b) of Fig. 1, whereas the field distribution from port 3 presents a multimode pattern [insets (c) and (d) of Fig. 1], consistent with the estimation based on parameter V of the fiber in the visible range.¹¹ The coupling efficiency at port 2 for 435-nm wavelength illumination is approximately 29%, with a splitting ratio of port 2 to port 3 of 99.6/0.4. The corresponding measurements for the 532-nm wavelength are 41% and 99.7/0.3, respectively. The reduction in the coupling efficiency at the wavelength of 435 nm may result from the greater loss of a higher mode [inset (c) of Fig. 1] at the coupler junction. The coupling measurements from port 1 to ports 2 and 3 show that the strength of the visible beams guided by the fiber coupler in the signal arm is 2 orders of magnitude higher than that in the excitation arm. As a result, the fiber coupler can act as a short-pass filter at a visible wavelength, which may optimize the delivery of a pulsed laser beam and the collected SHG signal.

The effectiveness of the fiber-optic SHG microscope is demonstrated by the SHG spectra from a thin layer of AF-50 dye. The layer is produced by evaporation

of a mixture of AF-50 dye and isopropyl alcohol on a coverslip with an average thickness of approximately 250 nm as measured by atomic-force microscopy. This dye, which has extended conjugated pi networks and aromatic heteroatom substitution, possesses large second-order and third-order nonlinear susceptibilities.¹² Therefore SHG and two-photon fluorescence can be produced simultaneously. In this case the femtosecond laser is scanned from 780 to 870 nm in wavelength, and the excitation polarization is parallel to the polarization of the incident laser. The emission spectra of AF-50 dye are collected by a spectrograph. As shown in Fig. 2, the emission spectrum with an excitation wavelength of 800 nm reveals a sharp SHG peak at 400 nm and a two-photon fluorescence lobe at wavelengths from 430 to 600 nm. For all the excitation wavelengths used, the SHG spectra peak at exactly half the excitation wavelengths and have the same bandwidth of approximately 10 nm, consistent with the excitation laser's spectral width. The SHG peak intensity is depicted in the inset of Fig. 2 as a function of excitation wavelength obtained with and without the fiber coupler. The increased SHG peak intensity propagated through the fiber coupler and detected by the spectrograph may arise from the increased SHG cross section of the AF-50 dye and the improved coupling efficiency of the fiber coupler in the visible range, as discussed in the previous paragraph. Figure 2 also implies that the simultaneous collection of SHG signal and two-photon fluorescence can be achieved efficiently through the fiber coupler, although second-harmonic and two-photon fluorescence occur in a much shorter wavelength region than the designed operating wavelength of the fiber coupler.

To investigate the optical sectioning ability of the fiber-optic SHG microscope we measured the axial response of the system¹³ to a thin layer, as described above. The dependence of the SHG peak intensity on the input power to port 3 of the coupler is shown in Fig. 3. It can be seen that the gradient of the log-log plot is 2.0 ± 0.1 , confirming the second-order

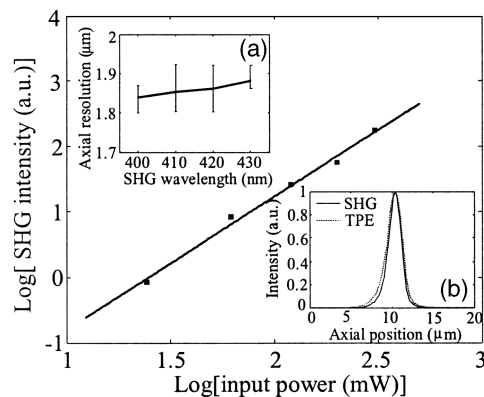


Fig. 3. Quadratic dependence of SHG peak intensity on excitation power: (a) FWHM of axial responses as a function of the SHG wavelength and (b) axial response of the system for SHG signal and two-photon-excited (TPE) fluorescence from a thin layer of AF-50 dye. The excitation wavelength is 800 nm.

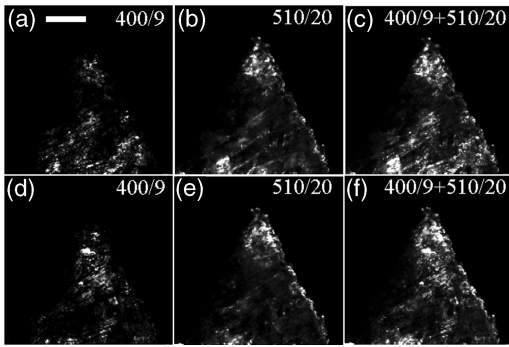


Fig. 4. SHG and two-photon fluorescence images of a triangle-shaped paper sheet excited by parallel polarization (top) and perpendicular polarization (bottom) beams at an 800-nm wavelength. The excitation power is approximately 4 mW on the sample. SHG images (a) and (d) were obtained with a 400/9-nm bandpass filter; two-photon fluorescence images (b) and (e), with a 510/20-nm bandpass filter. Images in (e) and (f) were obtained by overlaying the SHG and two-photon fluorescence image. Scale bar, 50 μm .

nonlinear frequency-conversion process. Inset (a) of Fig. 3 shows the FWHM of the SHG axial responses as a function of the detected SHG wavelength. Bandpass filters that have appropriate central wavelengths with a bandwidth of approximately 9 nm are placed before the PMT to collect the SHG signal. It is shown that the FWHM of the SHG axial responses varies from 1.8 to 1.9 μm as the excitation wavelength is tuned from 800 to 860 nm. In inset (b) of Fig. 3 the axial responses obtained with the SHG and two-photon fluorescence signals at an excitation wavelength of 800 nm are depicted. To record the two-photon fluorescence axial response we placed a 510/20 bandpass filter before the PMT to eliminate the second-harmonic and reflected fundamental wavelengths. Inset (b) of Fig. 3 reveals that the FWHM of these curves is approximately 1.8 and 2.1 μm , demonstrating that a slight improvement in resolution of approximately 14% for the SHG signal collection compared with the two-photon fluorescence axial response is obtained. This result is due to the fact that the SHG wavelength is shorter than the two-photon fluorescence wavelength.

To demonstrate the imaging capability and polarization sensitivity of the instrument, we measured the SHG and two-photon fluorescence images of a triangle-shaped sample excited by two beams of parallel and perpendicular polarization states. Usually SHG polarization anisotropy can be extracted by rotation of an analyzer before the detector or the input laser polarization.² As was demonstrated elsewhere,¹⁴ the fiber coupler shows the feature of linear polarization preservation along the birefringent axis from the near-infrared to the visible wavelength regions. The sample consists of a paper sheet (75 g/m²) with a mixture of AF-50 dye and isopropyl alcohol. The SHG and two-photon fluorescence images were obtained from the same sample site at the same focal plane

by use of 400/9- and 510/20-nm bandpass filters, respectively, as shown in Fig. 4. It can be seen that SHG and two-photon fluorescence microscopy do not produce exactly the same pattern of contrast. This property is caused by the different microscopic contrast mechanisms that can provide the complementary information shown in the overlay of the SHG and two-photon fluorescence images. Further observation of the SHG images shows that those with orthogonally polarized beam excitation display a distinguished appearance because the SHG signal arises from dipole interaction.

In conclusion, we have reported on the performance of a second-harmonic-generation microscope based on a single-mode fiber coupler in the excitation wavelength range from 780 to 870 nm. The fiber-optic SHG microscope reveals an axial resolution of approximately 1.8 μm , demonstrating an improvement in resolution compared with that which results from two-photon excitation. Both SHG and two-photon fluorescence images can be collected simultaneously through the new instrument under parallel and perpendicular excitation polarization of laser beams. Such multiple imaging modalities may prove advantageous in nonlinear optical endoscopy.

The authors thank the Australian Research Council for its support and Damian Bird for useful discussions and help. M. Gu's e-mail address is mgu@swin.edu.au.

References

1. Y. Guo, P. P. Ho, H. Savage, D. Harris, P. Sacks, S. Schantz, F. Liu, N. Zhadin, and R. R. Alfano, *Opt. Lett.* **22**, 1323 (1997).
2. P. J. Campagnola, A. C. Millard, M. Terasaki, P. E. Hoppe, C. J. Malone, and W. A. Mohler, *Biophys. J.* **81**, 493 (2002).
3. A. Zoumi, A. Yeh, and B. J. Tromberg, *Proc. Natl. Acad. Sci. USA* **99**, 11,014 (2002).
4. D. A. Dombeck, K. A. Kasichke, H. D. Vishwasrao, M. Ingelsson, B. T. Hyman, and W. W. Webb, *Proc. Natl. Acad. Sci. USA* **100**, 7081 (2003).
5. W. E. Zipfel, R. M. Williams, R. Christie, A. Y. Nikitin, B. T. Hyman, and W. W. Webb, *Proc. Natl. Acad. Sci. USA* **100**, 7075 (2003).
6. P. J. Campagnola and L. M. Loew, *Nat. Biotechnol.* **21**, 1356 (2003).
7. D. Bird and M. Gu, *Opt. Lett.* **27**, 1031 (2002).
8. D. Bird and M. Gu, *Opt. Lett.* **28**, 1552 (2003).
9. D. Bird and M. Gu, *Appl. Opt.* **41**, 1852 (2002).
10. D. Bird and M. Gu, *J. Microsc. (Oxford)* **208**, 35 (2002).
11. G. P. Agrawal, *Nonlinear Fiber Optics* (Academic, San Diego, Calif., 1989).
12. P. J. Campagnola, M. Wei, A. Lewis, and L. M. Loew, *Biophys. J.* **77**, 3341 (1999).
13. L. Liu, X. Deng, L. Yang, G. Wang, and Z. Xu, *Opt. Lett.* **25**, 1711 (2000).
14. L. Fu, X. Gan, D. Bird, and M. Gu, "Polarisation characteristics of a 1×2 fibre coupler under femtosecond pulsed and continuous wave illumination," *Opt. Laser Technol.* (to be published).